Investigation of the Effect of Finite Parallel Heat Transport on Magnetic Topology in 3-D Equilibria

Mark Schlutt and Chris C. Hegna
University of Wisconsin

Eric D. Held
Utah State University

Scott E. Kruger
Tech-X Corporation

Friday, 1 May 2009

Motivation.

- **Recent work indicates that in stellarators, stability may not limit β. Instead β may be limited by equilibrium physics.**[1] [2] [3] [4]
  - What maximum β is possible?
  - What factors and physics limit achievable β?
  - What equilibrium characteristics limit β?
- **The magnetic topology appears to change to limit β; flux surfaces deteriorate, enhancing transport.**
  - Pressure-induced currents may degrade magnetic surface integrity.
  - "Weakly stochastic" edge magnetic fields are produced, possibly as a result of self-consistent transport physics.

---

[1] M. Hirsch, et al., Plasma Phys. Control. Fusion, **50**, 1(2008).
[2] M. Sato, et al., 2008 IAEA Proceedings.
[3] A. Reiman, et al., Nucl. Fusion, **47**,572(2007)
[4] M.C. Zarnstorff, et al., 2004 IAEA Fusion Energy Conference.

Motivation and Thesis.

- **Finite transport along field lines is important to changes in the equilibrium magnetic topology. The ratio $\kappa_\parallel/\kappa_\perp$ may be related to maximum achievable β.**
  - Magnetic island physics is influenced by finite transport along field lines.[5] [6]
  - Stochastic regions have been observed to support a pressure gradient. [4]
- **GOAL: Study β-limiting phenomena, including the effect of self-consistent transport, using a resistive MHD model:**
  - **Analytically: Fully 3-D MHD equilibrium island width calculations, accounting for the effect of finite parallel heat conductivity. This work is on-going.**
  - **Numerically: Use the NIMROD code to study the magnetic field structure of straight stellarator configurations while varying $\kappa_\parallel/\kappa_\perp$.**

[5] R. Fitzpatrick, Phys. Plasmas, **2**, 825(1995).
[6] Gorenlenkov, et al., Phys. Plasmas, **3**, 3379(1996).

NIMROD is used to investigate magnetic topology in 3-D straight stellarator geometry.

MHD stability and MHD equilibrium island physics is studied in a self-consistently heated straight stellarator.

- Helically symmetric (2D) systems with good flux surfaces.
  - Heated system results should match solutions to the helically symmetric Grad-Shafranov equation. Opportunity to compare results with NIMROD's new module, nimeq.
  - Instability growth may result from **perturbing hot, helically symmetric systems**.
- Fully 3D systems.
  - **"Weakly stochastic" cases**, created by varying the magnitude of symmetry-breaking terms.
  - System is expected to exhibit changes in the magnetic topology which limit β, as it is heated.

NIMROD has been modified to allow modeling of a straight stellarator.

Code modifications completed to date:

- An **analytically prescribed** non-axisymmetric vacuum field is loaded into NIMROD's perturbed field representation.
- An ad-hoc heating source has been added to heat plasma near the geometric axis.
- The field line tracing code has been modified to calculate rotational transform for cases where the magnetic axis and geometric axis coincide.
- All above modifications function in either cylindrical or rectangular geometries.

The initial vacuum equilibrium magnetic field can be analytically prescribed.

Solving Laplace's equation in a periodic cylinder yields a scalar potential to describe the vacuum magnetic field for a straight stellarator:

$$\vec{B} = \nabla\phi$$

$$\phi = B_0 \left[R\zeta + \sum_{m,n \text{ pairs}} \epsilon_{mn} \frac{Rm}{n} I_m \left(\frac{nr}{R}\right) sin(m\theta - n\zeta) \right]$$

where:
$\epsilon_m = \frac{b_m}{B_0}$ is the relative amplitude of the helical harmonic of the magnetic field.
$I_m(x)$ is the modified bessel function of order m and argument x.

Magnetic field structure and spectrum are controlled by choice of ϵ_{mn}:

$$\iota \simeq \sum_{m,n} \frac{\epsilon_{mn}^2}{4} \left(\frac{1}{\rho}\frac{d}{d\rho}\right)^2 I_m^2(n\rho)$$

* Helically symmetric equilibria are a special subclass of solutions
  $\Longrightarrow \vec{B} = \vec{B}(\psi, M\theta - N\zeta)$

The boundary condition is a line-tied perfectly conducting shell.

- In general 3-D magnetic configurations, field lines intersect the computational boundary.
- After the analytic vacuum equilibrium is prescribed, a line-tied condition is enforced at the boundary. That is, the normal component of the magnetic field at the wall is NOT updated for t>0:

$$\frac{d}{dt}\vec{B}\cdot\hat{n}|_{bdry} = 0$$

This results in a vacuum magnetic field structure which persists in time, despite perturbations to the magnetic field.

This simulation is NEITHER a 'fixed boundary' nor a 'free boundary' simulation.

Straight Stellarator Parameters and Figures of Merit.

All calculations take place in straight stellarator geometry where:

a = minor radius $\simeq$ 0.4
B_0 = Guide field in axial direction = 1 T
T_{bckgrd} = background temperature (at plasma edge) = 1 eV
Kinematic viscosity = 0.01 m^2/s
Electrical Diffusivity $(\eta/\mu_0) = 1m^2/s$
τ_{res} = Resistive diffusion time = 0.16 s
τ_A = Alfven time = 6.4e-7 s
S = Lundquist number = 250,000
V_A = Alfven speed = 6.2e5 m/s
$\chi_\perp$ = perpendicular thermal diffusivity = 10 m^2/s
$\chi_\parallel$ = parallel thermal diffusivity = 1.0e8 m^2/s
P_m = magnetic Prantdl number = 0.01

NIMROD recognizes the prescribed analytical field as a valid vacuum solution.

- Good flux surfaces are observed to form for the case of the helically symmetric straight stellarator.
- Magnetic islands can be formed in vacuum by spoiling the helical symmetry. Stochastic regions can also be formed. To form magnetic islands, the additional symmetry-spoiling harmonics are chosen based on the rotational transform values.
- These vacuum solutions are seen to persist in time, even when subjected to large perturbations.
- For these heated cases, temperature contours closely match flux surfaces since parallel diffusivity is much greater than perpendicular diffusivity:

$$\frac{\chi_\perp}{\chi_\parallel} = \frac{10 \frac{m^2}{s}}{10^8 \frac{m^2}{s}} \tag{1}$$

Simulation conditions and general observations.

The m,n=2,2 helically symmetric vacuum magnetic field is used as a starting point. This system is evolved in time with various applied heating power and initial perturbations:

	Low Heating Power	High Heating Power
No initial perturbation	Flux surfaces remain intact with minor deformation.	Large flux surface deformation
Perturbed at t=0	Same as above - 'no initial perturbation'	Same as above - 'no initial perturbation'
Small Harmonic added to spoil 2D symmetry	Results pending	Results pending

Helically symmetric field: Good flux surfaces are initially formed.

m,n=2,2 helically symmetric magnetic field. **This is the starting point for all ensuing calculations.**

$$\vec{B} = \nabla\phi$$

$$\phi = B_0 \left[R\zeta + \sum_{2,2} \epsilon_{22} \frac{2R}{2} I_2 \left(\frac{2r}{R} \right) sin(2\theta - 2\zeta) \right]$$

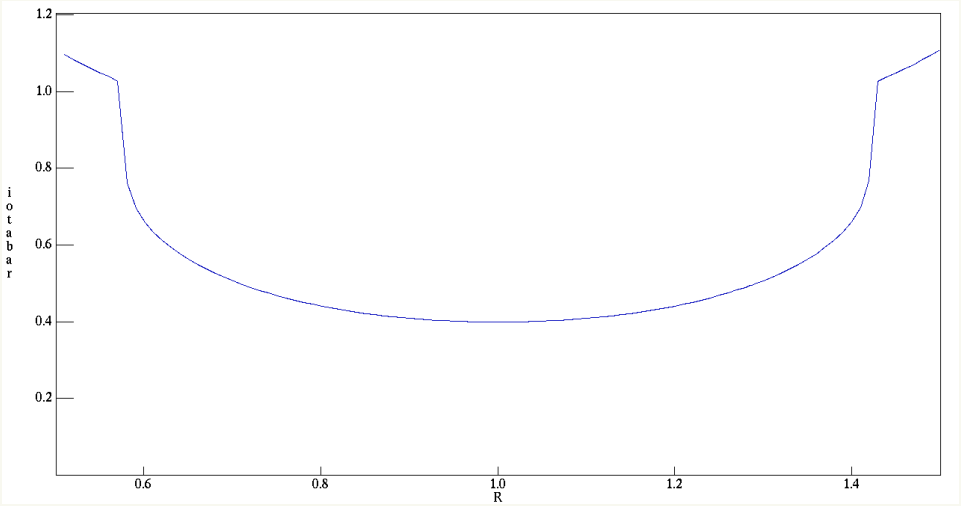

Figure 1: Rotational transform as a function of radius for m=2,n=2 at $\zeta = 0$.

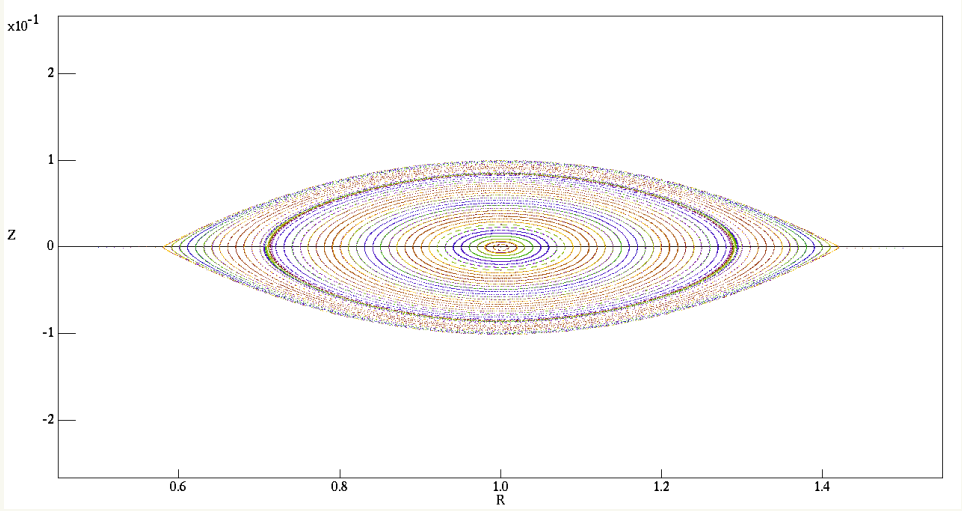

Figure 2: Poincare plot for m=2,n=2 at $\zeta = 0$.

Note: Periodic cylinder is 2π long.

Helically symmetric system with low heating power, $t = 6.972 \cdot 10^{-6}$s.

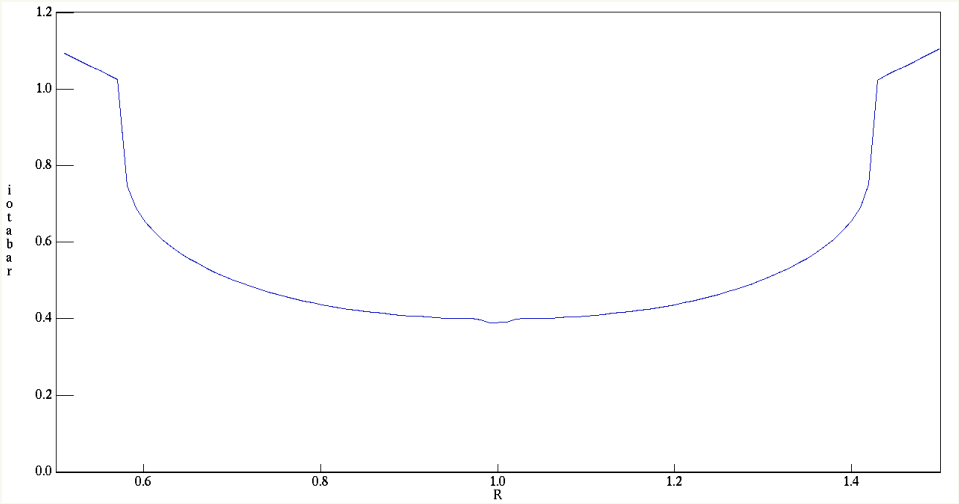

Figure 3: Rotational transform as a function of radius for m=2,n=2 at $\zeta = 0$.

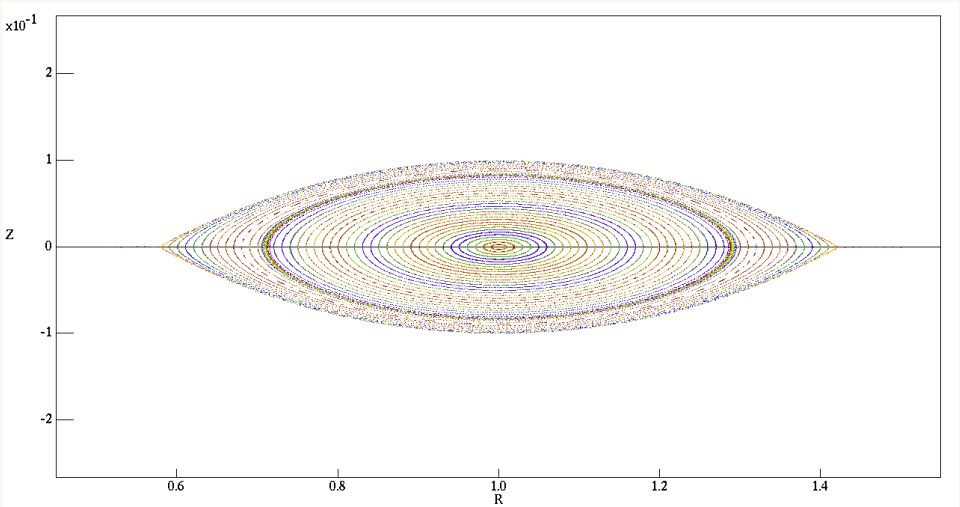

Figure 4: Poincare plot for m=2,n=2 at $\zeta = 0$.

Total $\beta = 0.4\%$. Local, on-axis $\beta = 10.7\%$.

THE UNIVERSITY of WISCONSIN MADISON

Helically symmetric system with low heating power, $t = 2.025 \cdot 10^{-5}$s.

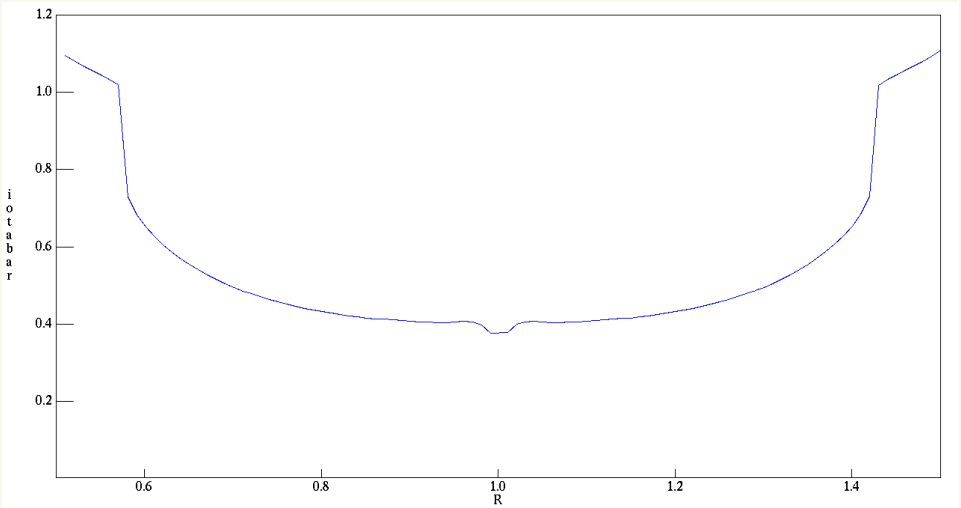

Figure 5: Rotational transform as a function of radius for m=2,n=2 at $\zeta = 0$.

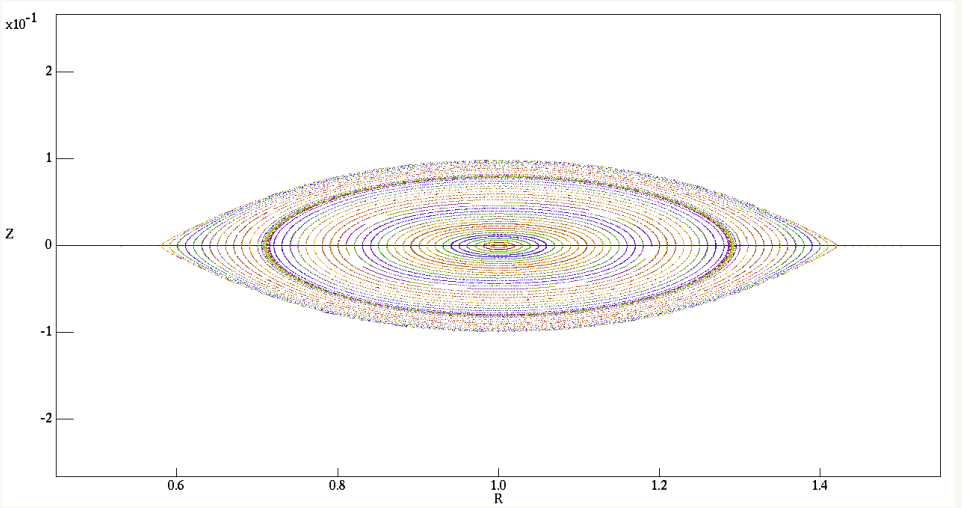

Figure 6: Poincare plot for m=2,n=2 at $\zeta = 0$.

Total $\beta = 0.9\%$. Local, on-axis $\beta = 34.8\%$.

THE UNIVERSITY of WISCONSIN MADISON

Helically symmetric system with LOW heating power, $t = 4.448 \cdot 10^{-5}$s.

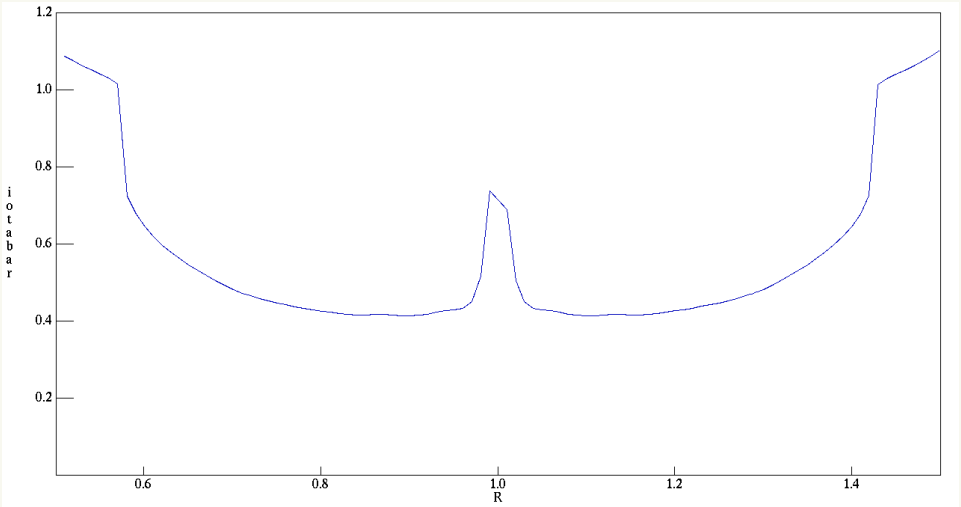

Figure 7: Rotational transform as a function of radius for m=2,n=2 at $\zeta = 0$.

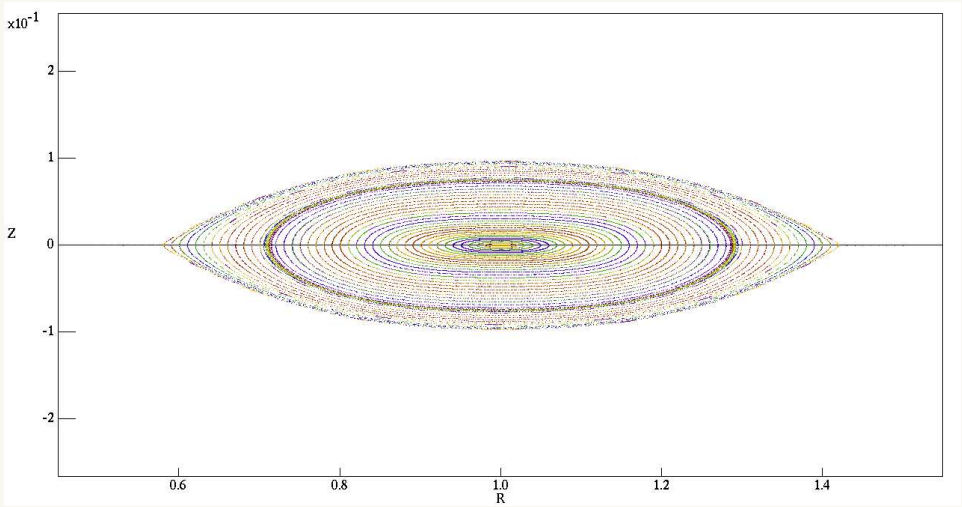

Figure 8: Poincare plot for m=2,n=2 at $\zeta = 0$.

Total $\beta = 1.4\%$. Local, on-axis $\beta = 68.2\%$.

Helically symmetric system with low heating power, summary

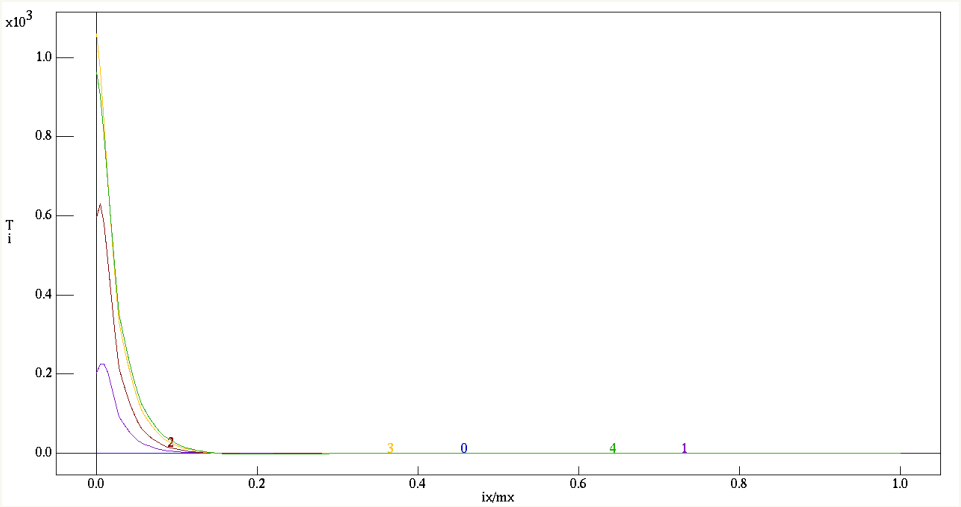

Figure 9: Temperature slices at $\zeta = 0$.

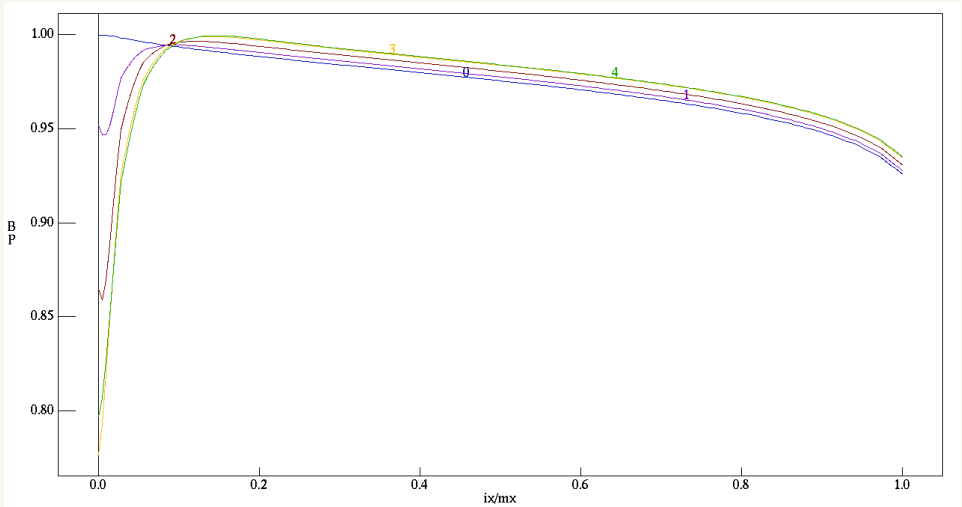

Figure 10: Axial magnetic field slices at $\zeta = 0$.

- In the absence of symmetry-spoiling perturbations, good flux surfaces are maintained; no flux surface destruction is observed.

Helically symmetric system with high heating power, $t = 4.508 \cdot 10^{-6}$s.

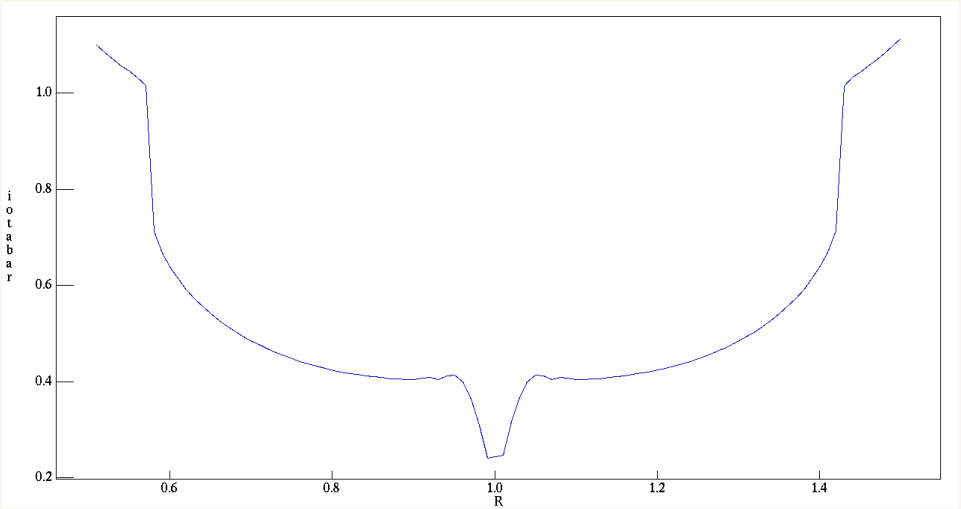

Figure 11: Rotational transform as a function of radius for m=2,n=2 at $\zeta = 0$.

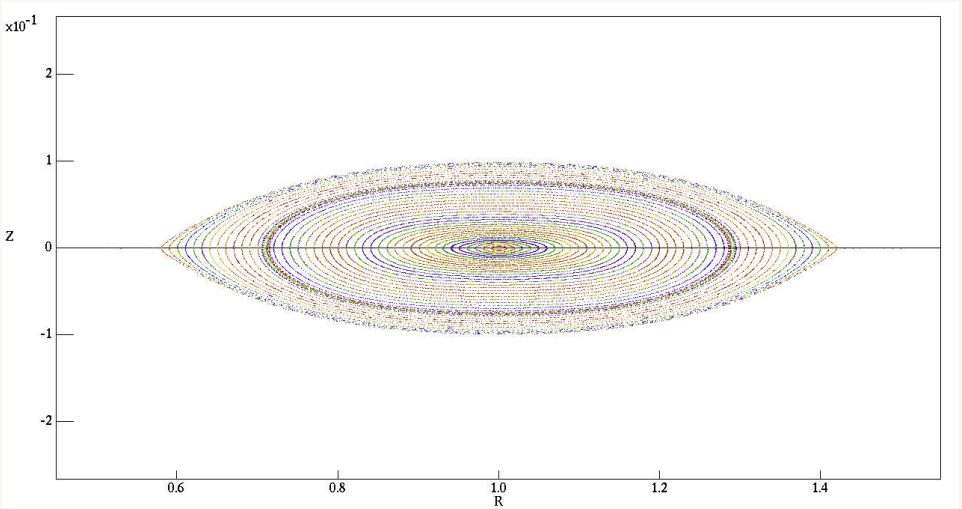

Figure 12: Poincare plot for m=2,n=2 at $\zeta = 0$.

Total $\beta = 2.1\%$. Local, on-axis $\beta = 72.8\%$.

THE UNIVERSITY of WISCONSIN MADISON

Helically symmetric system with high heating power, $t = 6.721 \cdot 10^{-6}$s.

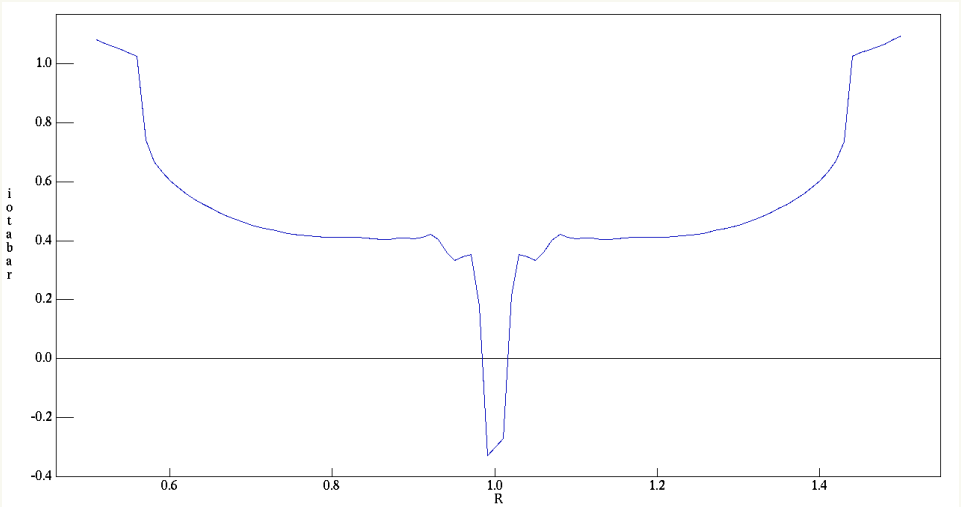

Figure 13: Rotational transform as a function of radius for m=2,n=2 at $\zeta = 0$.

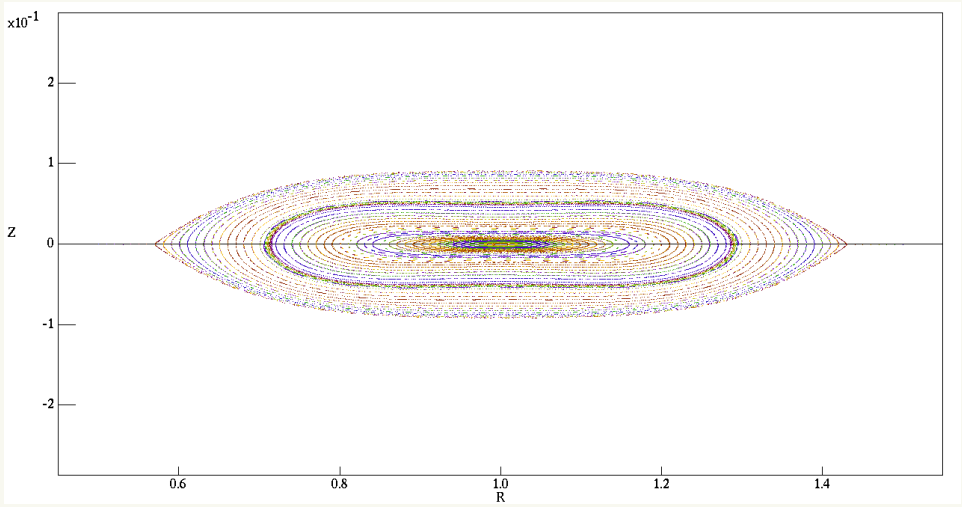

Figure 14: Poincare plot for m=2,n=2 at $\zeta = 0$.

Total $\beta = 3.1\%$. Local, on-axis $\beta = 126\%$.

THE UNIVERSITY of WISCONSIN MADISON

Helically symmetric system with high heating power, $t = 8.503 \cdot 10^{-6}$s.

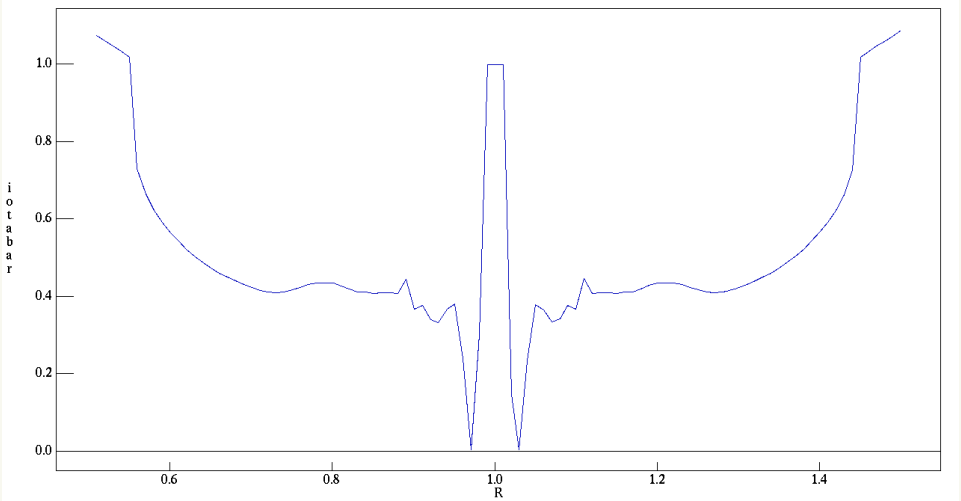

Figure 15: Rotational transform as a function of radius for m=2,n=2 at $\zeta = 0$.

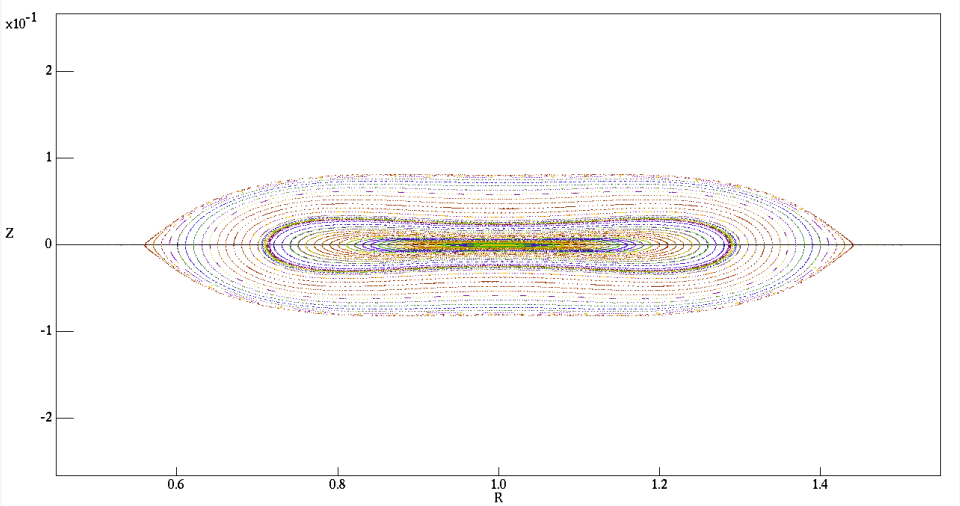

Figure 16: Poincare plot for m=2,n=2 at $\zeta = 0$.

Total $\beta = 3.4\%$. Local, on-axis $\beta = 81.5\%$.

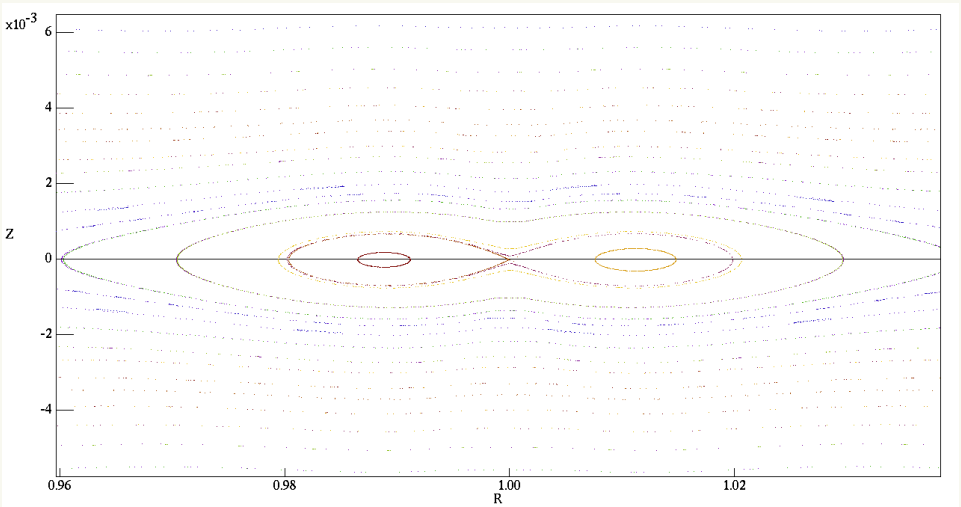

Figure 17: Poincare plot of core region.

THE UNIVERSITY of WISCONSIN MADISON

Helically symmetric system with HIGH heating power, summary

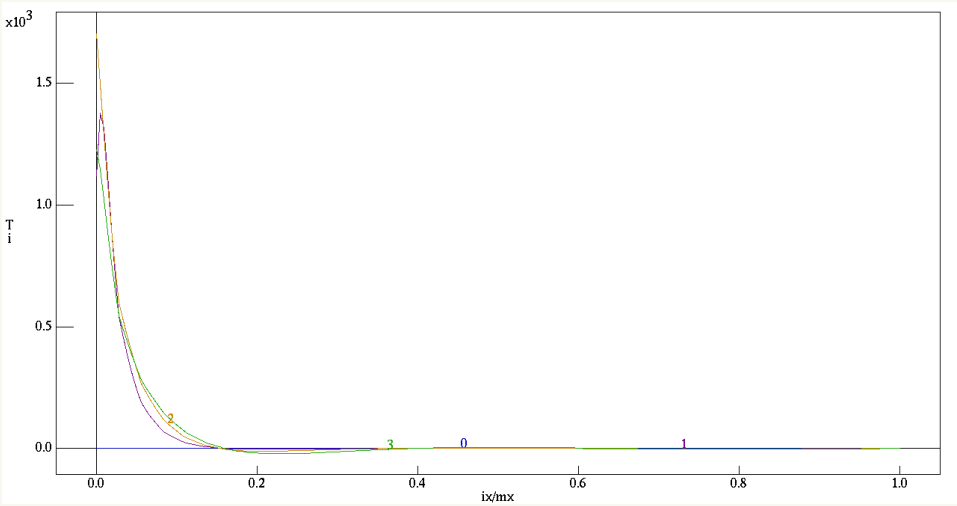

Figure 18: Temperature slices at $\zeta = 0$.

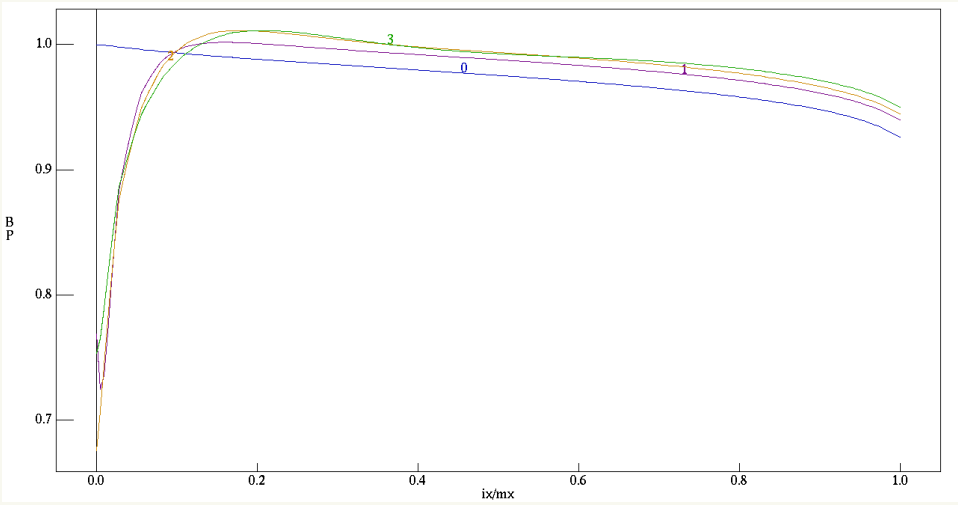

Figure 19: Axial magnetic field slices at $\zeta = 0$.

- In the absence of symmetry-spoiling perturbations, good flux surfaces are maintained; no flux surface destruction is observed.

Continuing and future work.

- It is thought that perhaps the heated, helically symmetric configurations shown on the previous slides could be above some MHD β limit and may be unstable. Next steps include using these configurations as a starting point and perturbing them to see if any instabilities manifest themselves.
- Is there an instability-induced β limit? Or is there gradual magnetic surface degradation?
  - Temperature evolution studies will continue for the two cases, helically symmetric (2-D) field and the broken symmetry (3-D) case.
  - Adjust the strength of the symmetry-breaking terms to obtain differing degrees of stochasticity.
  - The ratio $\frac{\kappa_\parallel}{\kappa_\perp}$ will be modified and the effect on β will be observed. Is the behavior related to standard stability metrics, e.g. Mercier criterion?
  - Investigate the physics of equlibrium island width as related to differing ratios of $\frac{\kappa_\parallel}{\kappa_\perp}$.
  - Possibility to compare contrast different heat transfer models. The present simulations use a local diffusive model for parallel heat transfer, $\vec{q} = \bar{\bar{\chi}} : \nabla T$. NIMROD has many possibilities to investigate this effect, ranging from constant thermal conductivities to temperature-dependent conductivities.

Summary of numerical results.

A 3-D magnetic field structure in a straight stellarator configuration has been modeled using NIMROD.

- In vacuum, good flux surfaces are formed by analytically prescribing the magnetic field structure.
  - These vacuum solutions persist in time, even when perturbed.
  - In vacuum, magnetic islands are formed by judicious addition of small harmonics.
- When the helically symmetric system is heated, good flux surfaces remain intact, but deform.